Desalination and Water Treatment
www.deswater.com

doi:10.5004/dwt.2017.20987

83 (2017) 244–252
July

Application of Doehlert matrix to determine the optimal conditions of Bromothymol Blue discoloration with Fenton process

Malak Maamar[a,b,*], Radouanne Fezei[c], Nebil Souissi[d], Nizar Bellakhal[a]

[a]Research Unit of Catalysis, Electrochemistry, Nanomaterials and their Applications and Didactic, National Institute of Applied Sciences and Technologies, Carthage University, 1080 Tunis, Tunisia, email: malakmaamar@hotmail.fr
[b]Department of Chemistry, Bizerte Faculty of Sciences, Carthage University, 7021 Zarzouna, Tunisia
[c]Valorization Laboratory of Useful Materials, National Center of Research in Materials Sciences, 8027 Soliman, Tunisia
[d]El Manar Preparatory Institute for Engineering Studies, El Manar University Campus, Tunis El Manar University, 2092 Tunis, Tunisia

Received 6 January 2016; Accepted 15 January 2017

ABSTRACT

The discoloration of a textile dye derivative bromothymol blue (BTB) in aqueous solution with Fenton process (FP) has been studied. The performance of the FP depends on various operating parameters such as the initial concentration of hydrogen peroxide $[H_2O_2]_0$, the initial ferrous ion concentration $[Fe^{2+}]_0$ and the pH of the reaction medium. The optimal conditions of these variables, for the discoloration of BTB with FP, have been investigated by the use of Doehlert matrix. It has been demonstrated that under the optimal conditions ($[H_2O_2]_0$ = 1.61 mM, $[Fe^{2+}]_0$ = 0.18 mM and pH = 2.85), FP leads to a maximum discoloration yield of BTB (67.58%± 4.39) after 1 h of treatment. These values were also experimentally validated. The obtained discoloration yield was 70.4%. After 6 h of BTB treatment in aqueous solution by FP, the color removal achievement was 91.54% and, the chemical oxygen demand (COD) removal reached 63%. Carboxylic acids and inorganic ions have been identified and followed during the mineralization of BTB with FP.

Keywords: Bromothymol blue; Fenton process; Discoloration; Experimental design methodology; Doehlert matrix

1. Introduction

Worldwide, textile wastewaters represent a big problem for conventional treatment plants. Annually, over 800000 tons of dyes are produced throughout the world [1,2]. It was indicating that approximately 15% of the synthetic textile dyes used is rejected in waste streams during manufacturing operations [3,4]. The release of these wastewaters into the environment is very dangerous to aquatic life [5] and mutagenic to human [6].

The issue of dyes removal from industrial effluents is receiving increasing attention as research area, as government legislation on the release of contaminated effluent is becoming increasingly stringent. The traditional physical techniques applied to treat textile wastewaters are mainly based on a phase transfer for the pollutant and have a fairly high cost of investment [7]. Furthermore, biological treatment is ineffective in the presence of toxic dyes due to the biological resistance and produces large quantities of sludge [7].

Hence, the orientation towards to advanced oxidation processes (AOPs), like Fenton process (FP), could be a good alternative to treat and eliminate textile dyes. This process appears to have the capacity to discolor and mineralize the textile industry dyes in short reaction time, as it was related by some studies [8–10].

In the past few years, the FP has been used to treat recalcitrant and toxic dyes and wastewaters [11–16]. This process

---

*Corresponding author.

Presented at the 5th Maghreb Conference on Desalination and Water Treatment — CMTDE 2015, December 21–24, 2015, Hammamet, Tunisia

employs ferrous ions and hydrogen peroxide under acidic pH conditions. As shown in Eq. (1), very strong oxidative hydroxyl radical ·OH is produced which allow complete discoloration of the dye until its total mineralization to H_2O, CO_2 and inorganic ions. This is due to the high oxidation potential ($E^0(\cdot OH/H_2O) = 2.8$ V/NHE) of the hydroxyl radicals [17,18].

$$Fe^{2+} + H_2O_2 \rightarrow Fe^{3+} + OH^- + \cdot OH \quad (1)$$

Bromothymol blue (BTB) also known as 3,3′-dibromothymolsulfonephtalein (Fig. 1), is a textile dye derivative, often deployed as a pH indicator [19,20]. Due to its wide spread application [21,22] and hazards associated with dyes in general (especially azo based dyes), its mineralization is considered as necessary. In order to decrease risks of its toxicity in wastewaters, the discoloration of this molecule until its mineralization were investigated by several authors [23–29]. To our knowledge, no one has systematically studied the discoloration of Bromothymol Blue by Fenton process using the experimental design methodology.

In the present work, the experimental design methodology [30] was used to investigate the influence of the principal experimental parameters (hydrogen peroxide initial concentration $[H_2O_2]_0$, ferrous ion initial concentration $[Fe^{2+}]_0$ and pH) on the efficiency of the FP for the discoloration of BTB and then determine the optimal conditions. It was used for planning the experimentation and analyzing the experimental results. It was noted that this methodology is then more effective and leads to a considerable reduction of the number of experiments and a fast results interpretation [31,32]. Under optimal conditions, mineralization of BTB by FP was followed. The color removal degree and the chemical oxygen demand (COD) removal percentage were determined. Inorganic ions and carboxylic acids were identified and quantified.

2. Materials and methods

2.1. Chemicals

BTB reagent was purchased from REACTIFS RAL. The chemical structure and the characteristics of BTB are given respectively in Fig. 1 and Table 1. Hydrogen peroxide (H_2O_2) 30% and heptahydrated ferrous sulfate ($FeSO_4{\cdot}7H_2O$), used as Fenton reagent, were supplied by VWR BDH Prolabo. Analytical grade diluted sulfuric acid (H_2SO_4) and sodium hydroxide (NaOH) were used to regulate the pH (Sigma-Aldrich). All the other chemicals were bought from Sigma-Aldrich.

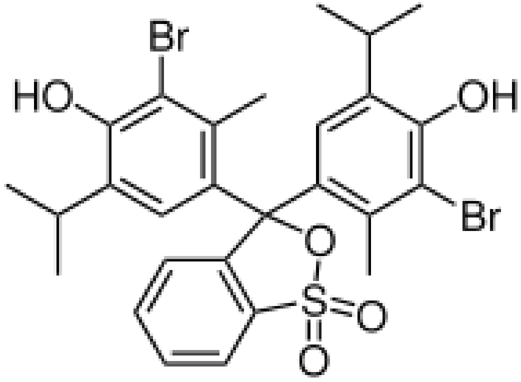

Fig. 1. Chemical structure of BTB.

2.2. Experimental procedure

Dye solution (1.6×10^{-4} M) was prepared using 100 mg BTB in 1 L distilled water. The experiments were performed in an open, undivided and cylindrical cell containing 250 mL of BTB synthetic solution. Solution pH values were adjusted to the desired level using dilute sulfuric acid (0.18 M) and sodium hydroxide (0.01 M), which were measured by a Mettler Toledo EL20 pH-meter. An appropriate amount of ferrous ion source was added to the solution. The reactions were initiated by adding hydrogen peroxide to the beaker. Samples were taken out from the beaker periodically and immediately analyzed.

2.3. Analytical determinations

2.3.1. Color removal measurements

The intensity of color removal was monitored by measuring the decrease in absorbance using Jouan VP1020 UV spectrophotometer at an absorbance detection of 433 nm which is the maximum wavelength of the acid form of BTB.

The color removal degree of the investigated solutions was determined using the following formula:

$$\%\ \text{Color removal} = \left(1 - \left(\frac{C_t}{C_0}\right)\right) \times 100 \quad (2)$$

where C_0 is the initial concentration of BTB and C_t is its concentration at treatment time t (min).

2.3.2. COD measurements

COD measurements were taken every 1 h of treatment, by sampling 2 mL of the treated solution. Aliquots of an acidic solution (1 mL) containing $K_2Cr_2O_7$ and $HgSO_4$ were added to the treated samples followed by the addition (3 mL) of concentrated H_2SO_4 containing $AgSO_4$. These solutions were heated at 150°C for 2 h in a COD block reactor to complete the oxidation of the remaining organic matter. Finally, the COD value was monitored using HANNA photometer COD.

Table 1
Characteristics of BTB

Characteristics	Data
Molecular formula	$C_{27}H_{28}Br_2O_5S$
Molecular weight (g mol^{-1})	624.381
Solubility in water (g L^{-1})	10

COD removal percentage was estimated using the following formula:

$$\% \, COD \text{ removal} = \left(1 - \left(\frac{COD_t}{COD_0}\right)\right) \times 100 \quad (3)$$

where COD_0 and COD_t are the measures of the chemical oxygen demand at reaction time (0 and t) of BTB Fenton treatment.

2.3.3. Ion chromatography

Generated inorganic ions were identified and quantified by DIONEX DX120 ion chromatography equipped with a conductivity detector, using an anion-exchange column AS18 (4 × 250 mm) as the stationary phase, and a solution of Na_2CO_3 (9 mM) in water as the mobile phase. The flow rate was set at 1 mL min^{-1}.

2.3.4. High performance liquid chromatography (HPLC)

The identification and the quantification of the carboxylic acids were monitored by thermo separation products (TSP) high performance liquid chromatography (HPLC) using Spectra system P1000, equipped with an isocratic pump and UV/Visible detector model Spectra series UV100, fitted with reversed phase C-18 analytical column Agilent (5 µm, 4.6 × 250 mm). The detection was performed at 210 nm with a mobile phase of 4 mM H_2SO_4 at a flow rate of 1 mL min^{-1}. The injection volume was 20 µL.

2.3.5. Doehlert experimental design

Doehlert experimental design [33] was used to determine the optimal operating conditions for the discoloration of BTB by FP. The influence of three factors (hydrogen peroxide initial concentration $[H_2O_2]_0$ (U_1), ferrous ion initial concentration $[Fe^{2+}]_0$ (U_2) and pH (U_3)) was studied. The response (Y) was the discoloration yield of BTB. The Doehlert design consists on N experiments with $N = K^2 + K + 1$, where K is the number of variables. For K = 3, the matrix comprised 13 experiments which were uniformly distributed within the space of the coded variables (X_i). The number of replicates of the center point was fixed at 6 (experiments 13–18) in order to obtain an estimation of the experimental error.

For the Doehlert experimental design construction, the retained domain for each variable was determined based on literature [34,35]. The experimental domain is summarized in Table 2.

The experimental response associated to the Doehlert matrix is represented by a quadratic polynomial model:

$$Y = b_0 + b_1X_1 + b_2X_2 + b_3X_3 + b_{11}X_1^2 + b_{22}X_2^2 + b_{33}X_3^2 + b_{12}(X_1X_2) + b_{13}(X_1X_3) + b_{23}(X_2X_3) \quad (4)$$

Where Y is the experimental response, b_0 is a constant of the model, b_i is the estimation of the main effects of the factor, b_{ii} is the estimation of the second order effects and b_{ij} is the estimation of the interactions between factors i and j.

Table 2
Experimental region investigated for BTB discoloration by FP

Variables	Factors	Unit	Center	Variation step
U_1	$[H_2O_2]$	mM	1.05	0.95
U_2	$[Fe^{2+}]$	mM	0.11	0.10
U_3	pH	–	3.50	1.50

The calculation of coefficients is carried out through the least squares method [36]:

$$B = (X^TX)^{-1}X^TY \quad (5)$$

where B is the vector of estimates of the coefficients, X is the model matrix, X^T is the transposed model matrix and Y is the vector of the measured response.

The transformation of natural variables (U_i) into coded variables (X_i) was made according to Eq. (6) [37]:

$$X_i = \left[\frac{U_i - U_{i(0)}}{\Delta U_i}\right] \quad (6)$$

where $U_{i(0)}$ is the value of U_i at the center of the study domain and ΔU_i is the variation step.

$$U_{i(0)} = \frac{\text{upper limit of } U_i + \text{lower limit of } U_i}{2} \quad (7)$$

$$\Delta U_i = \frac{\text{upper limit of } U_i - \text{lower limit of } U_i}{2} \quad (8)$$

The statistical significance of the model was checked using the variance analysis (ANOVA). The relationship between the response and the experimental variables was graphically illustrated by plotting the three-dimensional (3D) response surface and the two-dimensional (2D) iso-response curves. NEMRODW Software was used for data calculation and treatment.

3. Results and discussion

3.1. Optimal conditions for discoloration of BTB by FP

The performance of the FP depends on various operating parameters such as hydrogen peroxide initial concentration $[H_2O_2]_0$, ferrous ion initial concentration $[Fe^{2+}]_0$ and pH. The optimal conditions of these variables, for the discoloration of BTB by FP during 1 h, have been investigated by the use of Doehlert matrix. The Doehlert matrix experiments and experimental results are represented in Table 3.

The obtained responses (BTB discoloration yields (%)) were used to compute the polynomial model coefficients, leading to propose the following model equation:

$$Y = 47.11 + 9.63\,X_1 + 23.51\,X_2 - 13.96\,X_3 - 8.08\,X_1^2 - 12.37\,X_2^2 - 15.18\,X_3^2 + 5.01\,X_1X_2 - 9.69\,X_1X_3 + 1.24\,X_2X_3 \quad (9)$$

The negative coefficients for the model components X_3, X_1^2,X_2^2,$X_3^2$and X_1X_3 indicate the unfavorable effects on the BTB discoloration yield. While, the positive coefficients for

Table 3
Doehlert matrix experiments, experimental and calculated results for BTB discoloration by FP

Experiment number	Coded variables			Natural variables			Response BTB discoloration yields (Y (%))	
	X_1	X_2	X_3	$[H_2O_2]$ (mM)	$[Fe^{2+}]$ (mM)	pH	Experimental	Calculated
1	1.0000	0.0000	0.0000	2.00	0.11	3.50	53.52	48.66
2	–1.0000	0.0000	0.0000	0.10	0.11	3.50	24.54	29.40
3	0.5000	0.8660	0.0000	1.52	0.20	3.50	60.60	63.16
4	–0.5000	–0.8660	0.0000	0.58	0.02	3.50	15.37	12.81
5	0.5000	–0.8660	0.0000	1.52	0.02	3.50	14.32	18.11
6	–0.5000	0.8660	0.0000	0.58	0.20	3.50	52.98	49.19
7	0.5000	0.2887	0.8165	1.52	0.14	4.72	28.89	31.19
8	–0.5000	–0.2887	–0.8165	0.58	0.08	2.28	33.10	30.80
9	0.5000	–0.2887	–0.8165	1.52	0.08	2.28	45.82	46.89
10	0.0000	0.5774	–0.8165	1.05	0.17	2.28	56.03	57.26
11	–0.5000	0.2887	0.8165	0.58	0.14	4.72	29.11	28.04
12	0.0000	–0.5774	0.8165	1.05	0.05	4.72	8.54	7.31
13	0.0000	0.0000	0.0000	1.05	0.11	3.50	43.62	47.11
14	0.0000	0.0000	0.0000	1.05	0.11	3.50	44.74	47.11
15	0.0000	0.0000	0.0000	1.05	0.11	3.50	45.04	47.11
16	0.0000	0.0000	0.0000	1.05	0.11	3.50	47.59	47.11
17	0.0000	0.0000	0.0000	1.05	0.11	3.50	47.97	47.11
18	0.0000	0.0000	0.0000	1.05	0.11	3.50	53.72	47.11

X_1,X_2,X_1X_2 andX_2X_3 indicate favorable effects on the BTB discoloration yield.

The statistical significance of the second-order polynomial model to predict the BTB discoloration yields was tested by the analysis of variance (ANOVA). The ANOVA results given in Table 4 indicated that the fitted model presents a significant correlation with the experimental data (p-value < 0.1%). The best fit was also justified by a high value of the determination coefficient ($R^2 = 0.96$). This implies that 96% of the response variability was explained by the second-order polynomial predicted Eq. (9).

Consequently, we can conclude that the response Y is adequately described by the polynomial model, and that the generated regression Eq. (9) can be used to predict the Y-values in the studied domain. The BTB discoloration yields calculate by this equation are presented in Table 3. These results are in good agreement with the experimental values of BTB discoloration yields.

Fig. 2 shows iso-response curves and the corresponding three-dimensional representations associated to BTB discoloration yields as a function of the real and coded variables using Eq. (9). The graphic analysis of Fig. 2a and 2b shows that increasing hydrogen peroxide initial concentration and ferrous ion initial concentration enhanced the discoloration of BTB. This is due to an increased production of hydroxyl radicals. In addition, it could be noticed from Fig. 2c and 2d that when the initial concentration of hydrogen peroxide increases at an acidic pH (~ 3), the discoloration yield of BTB increases. It could be also noticed from Fig. 2e and 2f that when the pH of the reaction medium is approximately equal to 3 and the initial concentration of ferrous ion increases, the BTB discoloration yield increases.

Table 4
ANOVA results for BTB discoloration yields by FP

Source of variation	Sum of squares	Degrees of freedom	Mean square	F-ratio	p-value (%)
Regression	4037.88	9	448.654	20.9020	p < 0.1***
Residual	171.717	8	21.4647	–	–
Total	4209.60	17	–	–	–

*** Significant at 99.9% confidence level

Many studies have revealed that the solution pH can dramatically influence the discoloration of synthetic dyes in water by Fenton oxidation and the optimal solution pH values were approximately equal to 3 [38–41].

At low pH, the reaction according to Eqs. (10) and (11) could be slowed down because hydrogen peroxide can stay stable probably by solvating a proton to form an oxonium ion (Eq. (12)). An oxonium ion makes hydrogen peroxide electrophilic to enhance its stability and presumably to reduce substantially the reactivity with ferrous ion [42]. Simultaneously, the formed complex species $[Fe(H_2O)_6]^{2+}$ and $[Fe(H_2O)_6]^{3+}$ also react slower with hydrogen peroxide [43]. In addition, the scavenging effect of the $\cdot OH$ radical by H^+ is severe (Eq. (13)) [44,45].

$$Fe^{2+} + H_2O_2 + H^+ \rightarrow Fe^{3+} + \cdot OH + H_2O \tag{10}$$

$$Fe^{3+} + H_2O_2 \rightarrow Fe^{2+} + \cdot OOH + H^+ \tag{11}$$

$$H_2O_2 + H^+ \rightarrow H_3O_2^+ \tag{12}$$

$$\cdot OH + H^+ + e^- \rightarrow H_2O \tag{13}$$

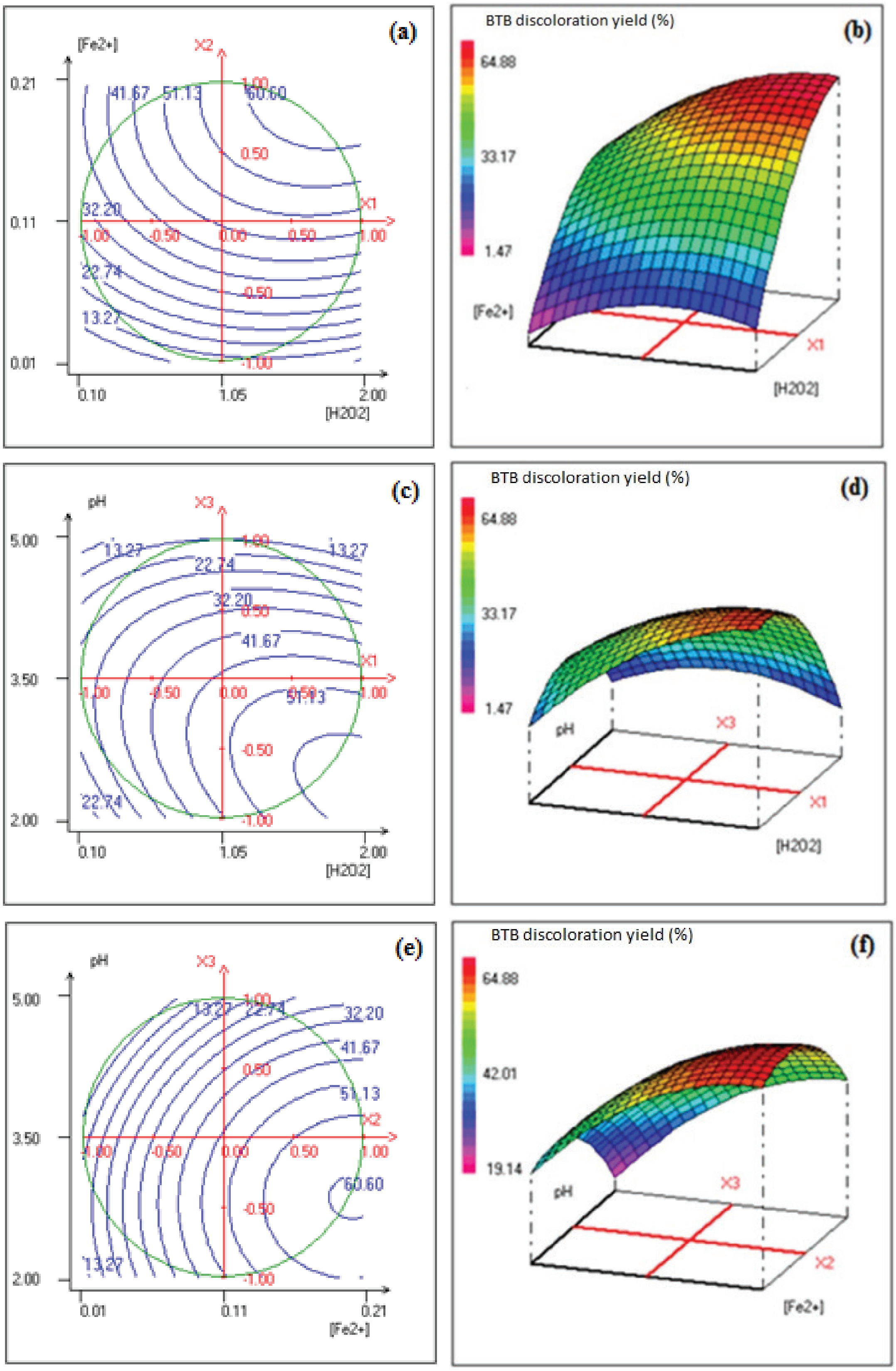

Fig. 2. (a) Contour plot of BTB discoloration yields vs. $[Fe^{2+}]_0$ (mM) and $[H_2O_2]_0$ (mM), (b) Corresponding 3D plot, (c) Contour plot of BTB discoloration yields vs. pH and $[H_2O_2]_0$ (mM), (d) Corresponding 3D plot, (e) Contour plot of BTB discoloration yields versus pH and $[Fe^{2+}]_0$ (mM), (f) Corresponding 3D plot.

In the case of pH higher than 4, the oxidation efficiency rapidly decreased, not only by decomposition of hydrogen peroxide but also by desactivation of the ferrous catalyst with the formation of ferric hydroxide complexes leading to a reduction of ·OH [46].

Moreover, the effect of increasing initial concentration of hydrogen peroxide from 0.1 to 1.61 mM was positive for the discoloration of BTB. This is due to the oxidation power of FP which improved with increasing ·OH amount in the solution resulting from the decomposition of an increasing amount of $[H_2O_2]_0$. But for a high initial concentration of hydrogen peroxide ($[H_2O_2]_0 > 1.61$ mM), the discoloration yield of BTB by FP decreases. This may be explained by the fact that the very reactive ·OH could be consumed by H_2O_2 and results in the generation of less reactive ·OOH radical (Eq. (14)) [47].

$$H_2O_2 + \cdot OH \rightarrow \cdot OOH + H_2O \tag{14}$$

It is important to control the initial concentration of hydrogen peroxide because the amount of H_2O_2 should be sufficient for the discoloration of BTB. In contrast a high concentration would be adverse to the discoloration of dye and would increase the cost of the dye treatment.

Furthermore, the discoloration yield of BTB increases when initial concentration of ferrous ion increases. This is due to the increase of ·OH production with the increase of $[Fe^{2+}]_0$ according to Eq. (10). Moreover, many studies have revealed that the use of a much higher concentration of Fe^{2+} (Eq. (15)) induces the decrease in discoloration yield of dyes [48].

$$\cdot OH + Fe^{2+} \rightarrow Fe^{3+} + OH^- \tag{15}$$

Based on the different results obtained previously, we were able to determine the conditions for a maximum BTB discoloration yield. The optimal values are shown in Table 5.

These values were experimentally validated. A discoloration yield of 70.41% was achieved after 1 h of BTB treatment by FP. This result confirms the maximum discoloration yield obtained by statistical calculations (Table 5). Indeed, statistically, the discoloration yield of BTB after 1 h of treatment by FP is equal to 67.58% with an error range of 4.39. This error of prediction is automatically generated by the NEMROD software. It is given by the following formula:

$$\sigma_{pred} = \sigma_R \text{ x } \sqrt{(d(Y_{pred}))} \tag{16}$$

where σ_{pred} is the error of the prediction value, σ_R the residual error and $d(Y_{pred})$ the prediction variance function at the considered experimental point.

Table 5
Optimal conditions for BTB discoloration by FP

Coded Variables	Factors	Coded values	Natural values	Discoloration yield of BTB (%)
X_1	$[H_2O_2]$ (mM)	0.591359	1.61	67.58 ± 4.39
X_2	$[Fe^{2+}]$ (mM)	0.678029	0.18	
X_3	pH	−0.436546	2.85	

Experimentally, the result obtained was 70.41% which confirms the statistical result because this value belongs to the interval [67.58–4.39 < experimental value found = 70.41 < 67.58 + 4.39].

3.2. Mineralization of BTB by FP

Mineralization of aqueous BTB synthetic solution was monitored by solution color intensity and COD abatement during FP treatment. These experiments were carried out under optimal operating conditions determined previously as described above in this work. Each experiment was carried out in triplicate and the values are reported average of three readings. The measurement uncertainly is 4.5%.

The evolution of the color removal percentage during the mineralization of BTB in aqueous solution by FP is shown in Fig. 3. A color removal of 91.54% was achieved after 6 h of treatment of BTB synthetic solution by FP. Similar observations were already reported for the mineralization of 20 different dyes by FP [49].

The evolution of the COD removal percentage during the mineralization of BTB in aqueous solution by FP is presented in Fig. 4. The initial COD value decreased quickly at the beginning of the treatment giving rise to a removal of more than 30% in only 1 h whereas the

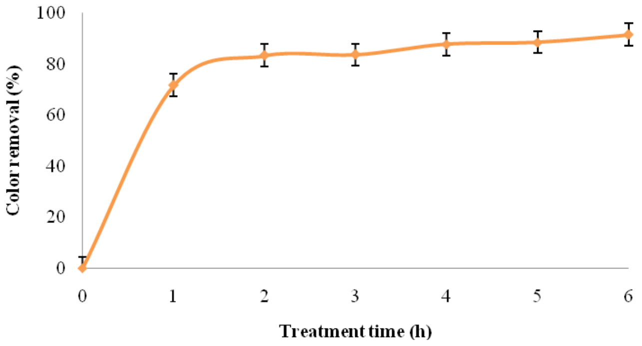

Fig. 3. Evolution of the color removal percentage of BTB synthetic solution treated with FP ($[H_2O_2]_0 = 1.61$ mM, $[Fe^{2+}]_0 = 0.18$ mM and pH = 2.85).

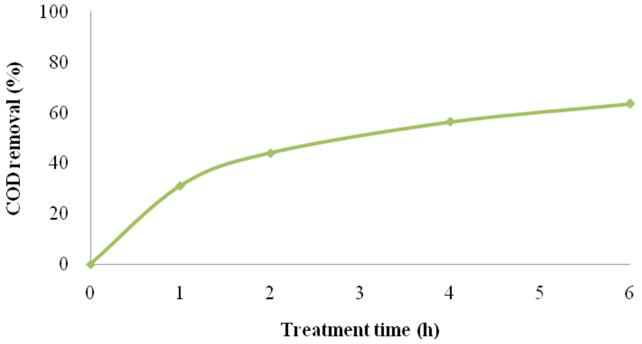

Fig. 4. Evolution of the COD removal percentage of BTB in aqueous solution treated by FP($[H_2O_2]_0 = 1.61$ mM, $[Fe^{2+}]_0 = 0.18$ mM and pH = 2.85).

removal gradually slows reaching a poor removal yield at the end of treatment. This is due to the formation of hardly oxidizable compounds such as short-chain carboxylic acids [50]. Nevertheless, an abatement of 63% of the initial COD value is reached at the end of 6 h of treatment. The final value of COD (44 mg O_2 L^{-1}) obtained complies with the Tunisian regulations (NT.106.002) for effluent discharges into the aquatic environment which sets a value of 90 mg O_2 L^{-1} for maritime public domain and public hydraulic areas and a value of 1000 mg O_2 L^{-1} for the utility pipes [51].

3.3. Identification of intermediates of BTB mineralization by FP

During the Fenton treatment, the oxidation reactions produced intermediates such as inorganic ions and carboxylic acids.

The BTB molecule contains an atom of sulfur (S) and two atoms of bromine (Br). Consequently, its mineralization by FP induced the progressive generation of inorganic ions such as sulphates (SO_4^{2-}) and bromides (Br^-). The results of the quantification of these inorganic ions are presented in Fig. 5. They show that the mineralization was accompanied by the conversion of its heteroatoms into inorganic ions. These ions started to be formed from the beginning of treatment and increased progressively as function of time. At the beginning of the mineralization of BTB by FP, bromides concentration was more important than that of sulphates. The final concentration of sulphates produced after 6 h of treatment reached a value of 5 mg L^{-1}. This value corresponds to 33% of the total sulphur of the initial molecule. The final concentration of bromides reached 9.92 mg L^{-1} which corresponds to 39% of the total bromine contained in the initial molecule. It may be explained by the presence of sulphates and bromides in some BTB intermediates structure [52,53].

Carboxylic acids are known to be the ultimate organic by-products of aromatic ring opening reactions [54]. In order to identify and follow the evolution of the carboxylic acids generated during the mineralization of BTB by FP, different standard solutions have been injected in the HPLC such as acetic acid, ascorbic acid, citric acid, formic acid, glycolic acid, oxalic acid and succinic acid. The carboxylic acids detected are acetic acid, formic acid, glycolic acid and oxalic acid (Table 6).

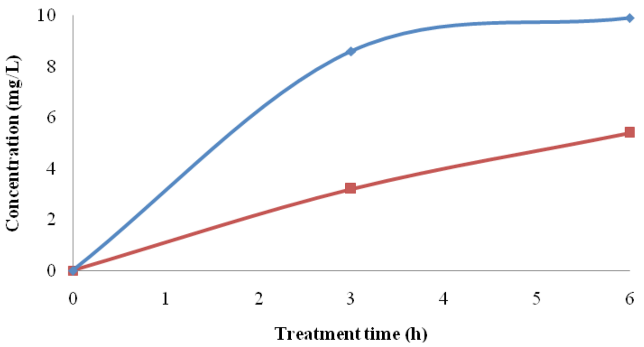

Fig. 5. Quantification of inorganic ions([H_2O_2]$_0$ = 1.61 mM, [Fe^{2+}]$_0$ = 0.18 mM and pH = 2.85), (☐) sulphates and (◊) bromides.

Acetic, glycolic and oxalic acid were identified at significant concentration and their evolution as function of treatment time is presented in Fig. 6, while formic acid was detected at a low concentration. As can be seen on Fig. 6, glycolic and acetic acid are generated as soon as the treatment is started reaching their maximum after 3 h. They disappeared completely respectively within 5 and 6 h. Although, oxalic acid decreased weakly with the treatment time, it remained present even at the end. This is due to the presence of stable ferric-oxalate complexes formed in the bulk, which are persistent and slowly destroyed by hydroxyl radicals [55].

The above results indicate that FP is effective to discolor as well aromatic compounds as aliphatics which are known as resistant to hydroxyl radical oxidation.

Table 6
The detected carboxylic acids during BTB mineralization with FP

Carboxylic acid	Molecular formula	Chemical structure
Acetic acid	$C_2H_4O_2$	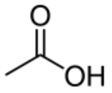
Formic acid	CH_2O_2	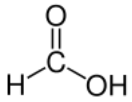
Glycolic acid	$C_2H_4O_3$	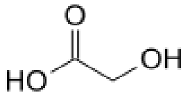
Oxalic acid	$C_2H_2O_4$	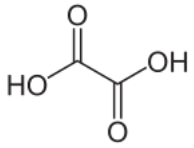

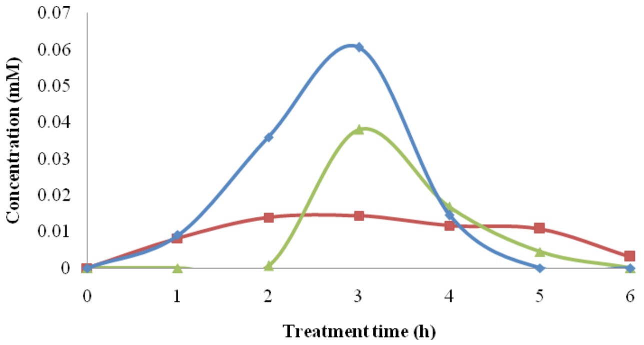

Fig. 6. Quantification of carboxylic acids([H_2O_2]$_0$ = 1.61 mM, [Fe^{2+}]$_0$ = 0.18 mM and pH = 2.85),(Δ) acetic acid, (◊) glycolic acid and (☐) oxalic acid.

4. Conclusions

In this study, we demonstrated that bromothymol blue, a textile dye derivative widely used in many areas, can be discolored in aqueous medium with FP. Indeed, 67.58% (± 4.39) of 100 mg L^{-1} of BTB was discolored in 1 h under optimal conditions ($[H_2O_2]_0$ = 1.61 mM, $[Fe^{2+}]_0$ = 0.18 mM and pH = 2.85) determined with Doehlert matrix. These values were also experimentally validated and the obtained discoloration yield was 70.4%.

Concerning the mineralization of the synthetic solution of BTB under optimal operating conditions, it was found that 91.54% of color removal and 63% of COD removal were achieved within 6 h of treatment by FP. Sulphates and bromides are the inorganic ions which appeared in BTB synthetic solution during its mineralization by FP. The carboxylic acids identified are acetic, formic, glycolic and oxalic acid.

The obtained results confirm that the treatment by FP is a good removal pathway for dyes because of its relatively low cost and efficiency without adding harmful chemical reagents to the solution to be treated. But, these results could be improved by coupling this process to another one.

References

[1] H. Zollinger, Color chemistry e syntheses, properties and applications of organic dyes and pigments, VCH Publishers, Cambridge, New York, 1991.
[2] N. Ben Hafaiedh, N. Bellakhal, Mineralization of synthetic and industrial food effluent containing Acid Red 18 by electro-Fenton process using a graphite-felt cathode, Int. J. Sci. Res. 4 (2015) 2643–2649.
[3] C. Maynard, Handbook of Industrial Chemistry,Van Nostrand Reinhold, New York, 1983.
[4] A.A. Vaidya, K.V. Datye, Environmental pollution during chemical processing of synthetic fibers, Colourage, 14 (1982) 3–10.
[5] K.T. Chung, S.E.J. Stevens, Degradation of azo dyes by environmental microorganisms and helminthes, Environ. Toxicol. Chem., 54 (1993) 435–441.
[6] K.T. Chung, S.E.J. Stevens, C.E. Cerniglia, The reduction of azo dyes by the intestinal microflora, Crit. Rev. Microbiol., 18 (1992) 175–197.
[7] M.S. Nawaz, M. Ahsan, Comparison of physico-chemical, advanced oxidation and biological techniques for the textile wastewater treatment, Alexandria Eng. J., 53 (2014) 717–722.
[8] S. Meric, D. Kaptan, T. O¨lmez, Color and COD removal from wastewater containing Reactive Black 5 using Fenton's oxidation process, Chemosphere, 54 (2004) 435–441.
[9] S.F. Kang, C.H. Liao, M.C. Chen, Pre-oxidation and coagulation of textile wastewater by the Fenton process, Chemosphere, 46 (2002) 923–928.
[10] M. Neamtu, A. Yediler, I. Siminiceanu, A. Kettrup, Oxidation of commercial reactive azo dye aqueous solutions by the photo-Fenton and Fenton-like processes, J. Photochem. Photobiol. A Chem., 141 (2001) 247–254.
[11] H. Gulyas, Processes for the removal of recalcitrant organics from industrial wastewaters, Water Sci. Technol., 36 (1997) 9–16.
[12] S.M. Kim, A. Vogelpohl, Degradation of organic pollutants by the photo-Fenton-process, Chem. Eng. Technol., 21 (1998) 187–191.
[13] S.F. Kang, T.H. Wang, Y.H. Lin, Decolorization and degradation of 2,4-dinitrophenol by Fenton's reagent, J. Enviorn. Sci. Health., A34 (1999) 935–950.
[14] E.G. Solozhenko, N.M. Soboleva, V.V. Goncharuk, Decolorization of azo dye solutions by Fenton's oxidation, Water Res., 29 (1995) 2206–2210.
[15] W.Z. Tang, R.Z. Chen, Decolorization kinetics and mechanisms of commercial dyes by H_2O_2/iron powder system, Chemosphere, 32 (1996) 947–958.
[16] S.F. Kang, C.H. Liao, H.P. Hung, Peroxidation treatment of dye manufacturing wastewater in the presence of ultraviolet light and ferrous ions, J. Hazard. Mater., B65 (1999) 317–333.
[17] H.J.H. Fenton, M.A., Oxidation of tartaric acid in the presence of iron, Chem. Soc. J. Lond., 65 (1894) 899–910.
[18] C. Walling, S. Kato, The oxidation of alcohols by Fenton's reagent: the effect of copper ion, J. Am. Chem. Soc., 93 (1971) 4275–4283.
[19] B.N. Chandrashekar, B.E. Kumara Swamy, K.R. Vishnu Mahesh, R.K. Umesh Chandra, B.S. Sherigara, Electrochemical studies of Bromothymol Blue at surfactant modified Carbon paste electrode by using cyclic Voltammetry, Int. J. Electrochem. Sci., 4 (2009) 471–480.
[20] G.E. Hoag, J.B. Collins, J.L Holcomb, J.R. Hoag, M.N. Nadagoudab, R.S. Varma, Degradation of bromothymol blue by greener nano-scale zero-valent iron synthesized using tea polyphenols, J. Mater. Chem., 19 (2009) 8671–677.
[21] A.M. Scheggi, F. Baldini, pH Sensing by Fibre Optics, Int. J. Opt., 33 (1986) 1587.
[22] J.C. Ibarra, A. Olivares-Perez, New holographic recording material: bromothymol blue dye with rosin, Opt. Mater., 20 (2002) 73.
[23] M.M. Haque, M. Muneer, TiO_2-mediated photocatalytic degradation of a textile dye derivative bromothymol blue in aqueous suspensions, Dyes Pigments, 75 (2007) 443–448.
[24] A. Doubla, L. Bouba Bello, M. Fotso, J.L. Brisset, Plasmachemical decolourisation of Bromothymol Blue by gliding electric discharge at atmospheric pressure, Dyes Pigments, 77 (2008) 118–124.
[25] S.H. Park, S.J. Kim, S.G. Seo, S.C. Jung, Assessment of microwave/UV/O_3 in the photo-catalytic degradation of bromothymol blue in aqueous nano TiO_2particles dispersions, Nanoscale Res. Lett., 5 (2010) 1627–1632.
[26] M. Kumar Sharma, M. Kumar Sharma, Photochemical treatment of bromothymol blue waste water by photo-Fenton reagent, Pollut. Res., 31 (2012) 319–324.
[27] P. Pradhan, R.J. Mascarenhas, T. Thomas, I.N.N. Namboothiri, O.J. D'Souza, Z. Mekhalif, Electropolymerization of bromothymol blue on carbon paste electrode bulk modified with oxidized multiwall carbon nanotubes and its application in amperometric sensing of epinephrine in pharmaceutical and biological samples, J. Electroanal. Chem., 732 (2014) 30–37.
[28] M. Maamar, I. Naimi, Y. Mkadem, N. Souissi, N. Bellakhal, Electrochemical oxidation of bromothymol blue: application to textile industrial wastewater treatment, J. Adv. Oxid. Technol., 18 (2015) 105–113.
[29] M. Bahrami, A. Nezamzdeh-Ejhieh, Effect of the supported ZnO on clinoptilolite nano-particules in the photodecolorization of semi-real sample bromothymol blue aqueous solution, Mater. Sci. Semicond. Process., 30 (2015) 275–284.
[30] G.A. Lewis, D. Mathieu, R. Phan-Tan-Luu, Pharmaceutical Experimental Design, Marcel Dekker, New York, 1998.
[31] F. Hellal, M. Dachraoui, Application of Doehlert matrix to the study of flow injection procedure for selenium (IV) determination, Talanta, 63 (2004) 1089–1094.
[32] J. Goupy, Selectivity of anion exchange membrane modified with polyethyleneimine, Techniques de l'ingénieur, Editions of T.I (ETI), vol. 4, France, pp. PE 230/1–PE 230/26.
[33] D.H. Doehlert, Uniform shell designs, J. Stat. Soc. Ser. C Appl. Stat., 19 (1970) 231–239.
[34] K. Zheng, C.Y. Lai, L.P. He, F. Li, Chromo-chemodosimetric detection for Fe^{2+} by Fenton reagent-induced chromophore-decolorizing of halogenated phenolsulfonphthalein derivatives, Sci. China Chem., 53 (2010) 1398–1405.
[35] M.S. Lucas, J.A. Peres, Decolorization of the azo dye Reactive Black 5 by Fenton and photo-Fenton oxidation, Dyes Pigments, 71 (2006) 236–244.

[36] S. Hammami, A. Ouejhani, N. Bellakhal, M. Dachraoui, Application of Doehlert matrix to determine the optimal conditions of electrochemical treatment of tannery effluents, J. Hazard Mater., 163 (2009) 251–258.

[37] D. Mansour, F. Foucarde, I. Soutrel, D. Hauchard, N. Bellakhal, A. Amarane, Mineralization of synthetic and industrial pharmaceutical effluent containing trimethoprim by combining electro-Fenton and activated sludge treatment, J. Taiwan Inst. Chem. E., 000 (2015) 1–10.

[38] C. Walling, Fenton's reagent revisited, Acc. Chem. Res., 8 (1975) 125–131.

[39] N. Kang, D.S. Lee, J. Yoon, Kinetic modeling of Fenton oxidation of phenol and monochlorophenols, Chemosphere, 47 (2002) 915–924.

[40] G. Ghiselli, W.F. Jardim, M.I. Litter, H.D. Mansilla, Destruction of EDTA using Fenton and photo-Fenton-like reactions under UV-A irradiation, J. Photochem. Photobiol. A Chem., 167 (2004) 59–67.

[41] M.M. Hassan, C.J. Hawkyard, Decolorization of aqueous dyes by sequential oxidation treatment with ozone and Fenton's reagent, J. Chem. Technol. Biotechnol., 77 (2002) 834–841.

[42] B.G. Kwon, D.S. Lee, N. Kang, J. Yoon, Characteristics of p-chlorophenol oxidation by Fenton's reagent, Water Res., 33 (1999) 2110–2118.

[43] S.H. Bossmann, E. Oliveros, S. Gob, S. Siegwart, E.P. Dahlen, L.J. Payawan, New evidence against hydroxyl radicals as reactive intermediates in the thermal and photochemically enhanced Fenton reactions, J. Phys. Chem. A., 102 (1998) 5542–5550.

[44] J. Feng, X. Hu, P.L. Yue, H.Y. Zhu, G.Q. Lu, Degradation of azo-dye orange II by a photo-assisted Fenton reaction using a novel composite of iron oxide and silicate nanoparticles as a catalyst, Ind. Eng. Chem. Res., 42 (2003) 2058–2066.

[45] M. Muruganandham, M. Swaminathan, Decolorization of Reactive Orange 4 by Fenton and photo-Fenton oxidation technology, Dyes Pigments, 63 (2004) 315–321.

[46] J.H. Sun, S.P. Sun, G.L. Wang, L.P. Qiao, Degradation of azo dye Amido black 10B in aqueous solution by Fenton oxidation process, Dyes Pigments, 74 (2007) 647–652.

[47] R. Chen, J.J. Pignatello, Role of quinone intermediates as electron shuttles in Fenton and photo-assisted Fenton oxidations of aromatic compounds, Environ. Sci. Technol., 31 (1997) 399–406.

[48] J.M. Joseph, H. Destaillats, H.M. Hung, M.R. Hoffmann, The sonochemical degradation of azobenzene and related azo dyes: rate enhancements via Fenton's reactions, J. Phys. Chem. A., 104 (2000) 301–307.

[49] X.R. Xu, H.B. Li, W.H. Wang, J.D. Gu, Degradation of dyes in aqueous solutions by the Fenton process, Chemosphere, 57 (2004) 595–600.

[50] M.A. Oturan, M. Pimentel, N. Oturan, I. Sirés, Reaction sequence for the mineralization of the short-chain carboxylic acids usually formed upon cleavage of aromatics during the electrochemical Fenton treatment, I. Electrochim. Acta., 54 (2008) 173–182.

[51] Tunisian standard NT.106.002 (1989) on the discharge of effluent into the aquatic environment (Environmental Protection), Standard approved by decree of the Minister of Economy of 20 July 1989, JORT n^{0}59, 1332.

[52] S. Hammami, N. Oturan, N. Bellakhal, M. Dachraoui, M.A. Oturan, Oxidative degradation of direct orange 61 by electro-Fenton process using a carbon felt electrode: Application of the experimental design methodology, J. Electroanal. Chem., 610 (2007) 75–84.

[53] C. Annabi, F. Foucarde, I. Soutrel, F. Geneste, D. Floner, N. Bellakhal, A. Amrane, Degradation of enoxacin antibiotic by the electro-Fenton process: Optimization, biodegradability improvement and degradation mechanism, J. Environ. Manage., 165 (2016) 96–105.

[54] M.A. Oturan, J. Peiroten, P. Chartrin, A.J. Acher, Complete destruction of p-nitrophenol in aqueous medium by electro-Fenton method, Environ. Sci. Technol., 34 (2000) 3474–3479.

[55] I. Naimi, M.R. Louhaichi, M.C. Ben Rayana, N. Bellakhal, Electrochemical Advanced Oxidation of 4, 4′-Sulfonyldiphenol on BDD and Pt Anodes in Aqueous Medium, Int. J. Eng. Res. Technol., 3 (2014) 436–442.